NJC

PAPER

The effect of reaction atmosphere and growth duration on the size and morphology of boron nitride nanotubes†

Pervaiz Ahmad,[a] Mayeen Uddin Khandaker,*[a] Yusoff Mohd Amin,[a]
Nawshad Muhammad,[b] Ahmed Rufai Usman[a] and Muhammad Amin[c]

The effect of different reaction atmospheres is analyzed on the size and morphology of boron nitride nanotubes within a single and continuous growth duration of 180 min at 1200 °C. Field emission scanning electron microscopy micrographs show smaller and larger diameter boron nitride nanotubes in the range of 70–700 nm, with straight and curve parts. Some of the larger diameter boron nitride nanotubes have pipe-like morphologies at their top with the diameter in the range of 270–380 nm. High resolution transmission electron microscopy shows the tubular structure of the synthesized nanotubes with a non-uniform diameter. X-ray photoelectron spectroscopy shows B1s and N1s peaks at 190.3 eV and 398 eV for hexagonal boron nitride nature of the synthesized nanotubes. The Raman spectrum reports a higher intensity peak at 1370 (cm^{-1}) that corresponds to E_{2g} mode of vibration in hexagonal boron nitride.

1. Introduction

The discovery of carbon nanotubes (CNTs)[1] is one of the major breakthroughs in developing tubular morphologies at nanoscale (10^{-9}) dimensions. CNTs have exceptional electrical and mechanical properties that have made them suitable candidates for different applications in the real world. However, CNTs have diameter dependent electronic properties which have made them unsuitable for making devices with uniform electronic properties.[2]

Boron nitride nanotubes (BNNTs) are the structural analogs of CNTs. They were theoretically predicted from the elemental composition of boron (B) and nitrogen (N) in 1994[3] and experimentally synthesized with hexagonal boron nitride (h-BN) nature in 1995.[4] Like their structural analog (CNTs), BNNTs have excellent properties. These properties include the diameter independent electronic properties. In this sense, BNNTs have fulfilled the demands of the materials with uniform electronic properties which were otherwise not possible with CNTs.[2]

[a] *Department of Physics, Faculty of Science University of Malaya, 50603 Kuala Lumpur, Malaysia. E-mail: mu_khandaker@yahoo.com, mu_khandaker@um.edu.my; Fax: +60379674146; Tel: +601115402880*

[b] *Interdisciplinary Research Centre in Biomedical Materials (IRCBM), COMSATS Institute of Information Technology, 54000 Lahore, Pakistan*

[c] *Department of Physics, University of the Punjab, Quaid-e-Azam Campus, 54590 Lahore, Pakistan*

† 81.07.De

The research on the BNNTs has revealed their potential applications in the field of bio-medical, microelectronic mechanical systems[5,6] and in solid state neutron detectors.[7] They are found to be a useful material for changing the optical properties of materials,[8,9] hydrogen storage applications[10–14] and increasing superplasticity of engineering ceramics.[15]

Prior to be utilized in any of their potential applications, BNNTs need to be synthesized not only in good quality and large quantity but also in proper size and morphology. In this regard, the roles of certain parameters are very important during the synthesis of BNNTs for controling their size and morphologies along with the quality and quantity of the final product.[16] These parameters include: precursor type, precursor ratio, temperature, reaction atmosphere, growth duration, catalysts and substrate type.[16] B, MgO and γ-Fe$_2$O$_3$ are proved to be the most effective precursors for the BNNT synthesis.[17] The 2:1:1 ratio of these precursors is used to produce high quality BNNTs.[18] The reduction of the growth duration (from 60 to 30 min), change in the precursor ratio (from 2:1:1 to 4:1:1) and substrate (with deposited catalysts) nature causes the pattern growth of the BNNTs.[19] The same precursors (B, MgO and γ-Fe$_2$O$_3$) in different weight ratios and at different temperatures (1200, 1300 and 1400 °C) have produced BNNTs of different sizes and morphologies.[20] The change of the reaction atmosphere to Argon gas instead of vacuum or evacuation has resulted in the synthesis of boron nitride nanowires (BNNWs) in a growth duration of 30 min[16] and BNNTs in a growth duration of 70 min[21] whereas the change in the reaction atmosphere to NH$_3$ instead of

vacuum/evacuation or Argon gas has resulted in the synthesis of boron nitride microtubes (BNMTs) and the formation of boron nitride nanosheets (BNNS) within a growth duration of 60 min.[22] It has also been noted that an increase in growth duration (from 60 to 90 min) under the same circumtances has produced only BNNS from B, MgO and γ-Fe$_2$O$_3$ as precursors.[23]

It has been observed that the change in temperature and precursor ratio results in a change in size and morphology of the BNNTs[20] whereas the change of the reaction atmosphere not only effect the size and morphology of BNNTs but also provides options for the synthesis of BNNWs,[16] BNMTs and BNNS.[22]

After changes have been observed in the type, size and morphology of nanostructured h-BN on the basis of the reaction atmosphere and growth duration it was decided to use different reaction atmosphere within a single experiment and find their effects on the type, size and morphology of the final product.

2. Materials and methods

Nanoscale powders of B, MgO and γ-Fe$_2$O$_3$ are mixed in a 2 : 1 : 1 ratio as precursors for the synthesis of BNNTs in the present study. This mixture of nano-precursors with a total weight of 200 mg is taken in an alumina boat and partially covered with a few Si substrates. The conventional horizontal quartz tube furnace with one end closed inner quartz tube is used as the experimental set up. Before the experiment, the experimental set up is flushed with Argon gas. Afterward, the precursors are heated up to 1200 °C at a heating rate of 10 °C min^{-1}. Argon gas at a flow rate of 200 sccm provides an inert atmosphere during the heating process from room temperature up to 1200 °C. When the temperature reached 1200 °C, argon gas flow is stopped and NH$_3$ gas flow is introduced into the system at a flow rate of 200 sccm. The temperature of the system and the flow of NH$_3$ gas in the system are maintained in such a condition for 3 h. After 3 h, NH$_3$ gas flow is switched off and the system is again brought to room temperature in the same inert atmosphere of Argon gas.

At room temperature, the sample is collected from the system and characterized with the help of different characterization instruments to study the surface morphology, internal structure and constituents of the synthesized sample.

3. Results and discussion

BNNTs are synthesized in different reaction atmospheres within a growth duration of 180 min at 1200 °C to study their effect on the size and morphology of the final product. Scanning electron microscopy (FESEM), High resolution transmission electron microscopy (HR-TEM), X-ray photoelectron spectroscopy (XPS) and Raman spectroscopy are used to characterize the as-synthesized BNNTs.

Fig. 1 shows different magnifications of FESEM micrographs of the BNNTs synthesized in the present study. Fig. 1(a) shows the low magnification top view of the BNNTs. The top view shows partially vertically aligned BNNTs with curved morphology.
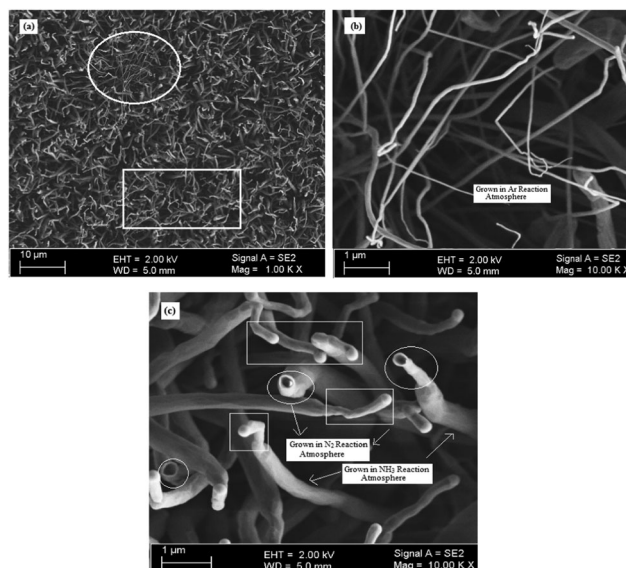

Fig. 1   FESEM (a) low magnification top view of the whole BNNT sample. (b) High magnification micrograph of the BNNT portion grown in the presence of Argon gas as a reaction atmosphere. (c) High magnification micrograph of the BNNT portion grown in the presence of NH$_3$ as a reaction atmosphere. BNNT morphologies above the knot like structure (indicated with circles and reactangles) are formed due to the presence of N$_2$ as the reaction atmosphere.

BNNTs of different sizes or diameters can be seen in the current micrograph. These different sizes and morphologies of the BNNTs are indicated with the help of a white circle and rectangle in Fig. 1(a) and separately shown in the magnified form (higher magnification) in Fig. 1(b) and (c). The portion of smaller diameter BNNTs indicated in Fig. 1(a) with the help of a white circle is shown in higher magnification in Fig. 1(b). These smaller size BNNTs are found to have diameter in the range of 70–130 nm and most probably have grown in the presence of the Argon reaction atmosphere. The micrograph shows curve morphologies of the BNNTs with some straight parts. Some of the BNNTs are thoroughly curved whereas some of the tubes are straight from some parts and curved or bended at the ends or middle. Fig. 1(c) shows the higher magnification micrograph of the BNNT portion specified in Fig. 1(a) via a white retangle. The diameter of these BNNTs can be found in the range of 70–700 nm. These large diameter BNNTs are believed to have formed in the presence of NH$_3$ as the reaction atmosphere.[22] The straight and curve parts of the BNNTs can clearly be seen at this magnification. Along with straight and curly morphologies, change in the diameter (from bottom to top) of the BNNTs can also be observed.[24] An irregular decrease and increase in the diameter of the BNNTs can be found from bottom to top untill a certain point with a knot like structure. From knot like structure onwards some of the BNNTs have a clear pipe-like structure with an opened end from the top. These BNNTs are indicated with the help of white circles in Fig. 1(c). The diameter of these open ends can be found in the range of 270–380 nm. Some more BNNTs with the same morphology (and diameter) but with a closed top end can also be seen along
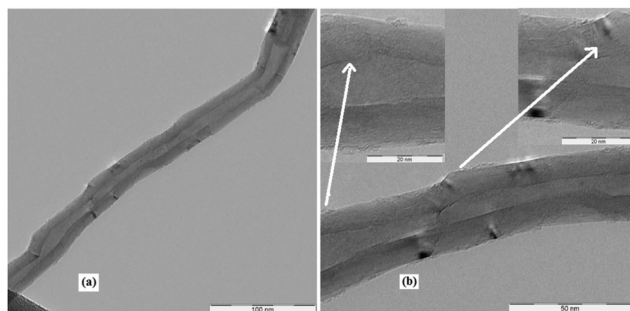
Fig. 2 (a) Low resolution TEM micrograph of the BNNT shows irregular external and internal diameters of the tube. (b) High resolution micrograph of the same BNNTs confirms the irregular diameter of the BNNT. The insets show higher resolution micrographs of the curve parts of the BNNT indicated by arrows.
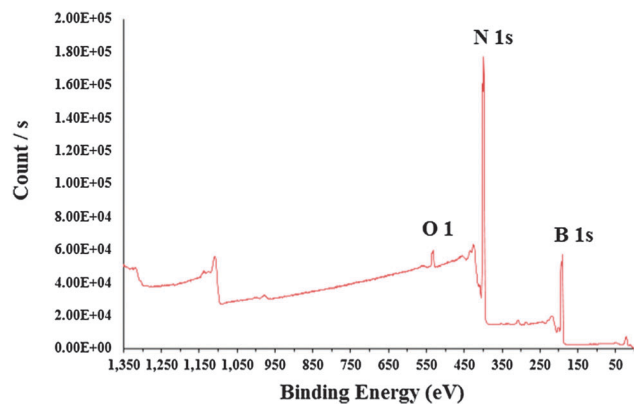

Fig. 3 XPS survey shows B1s peak at 190.3 eV and N1s peak at 398 eV for the h-BN nature of the BNNTs.
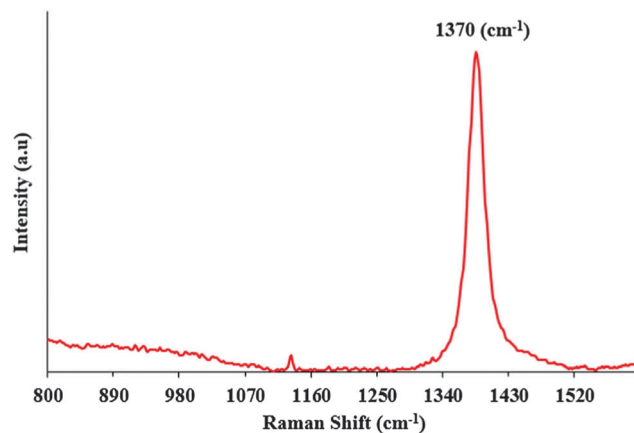

Fig. 4 Raman spectrum shows major peaks at 1370 (cm^{-1}) for h-BN compositions of the synthesized BNNTs in the sample.

with others (with an open top) indicated by white reactangles. These BNNTs have curve or bending morphology above the knot point and constitute the major part of the sample. The portions of these BNNTs (indicated with white circles and reactangles) might have formed when N_2 from NH_3 decomposition provides the reaction atmosphere.

The internal structure of the BNNTs is examined with the help of a transmission electron microscope (TEM). The observation of the internal structure of the as-obtained BNNTs in the form of TEM micrographs is shown in Fig. 2. Fig. 2(a) is the low resolution TEM micrograph of the BNNTs that reports not only the external but also the internal irregular diameter of the tube. Furthermore, the micrograph shows the curve morphology of the BNNT with an internal bamboo like structure. Fig. 2(b) shows the high resolution micrograph of the same BNNTs. The irregularity in the internal diameter of the BNNT can be clearly seen at this resolution. The most irregular part of the BNNT with respect to internal and external diameters is indicated with the help of white arrows and magnified in high resolution micrographs shown in the inset of Fig. 2(b). The curve morphology and irregularity observed in the BNNT diameter *via* TEM confirms the BNNT morphology shown in Fig. 1 with the help of FESEM micrographs.

X-ray photoelectron spectroscopy (XPS) is employed to characterize the synthesized BNNT sample for its Boron (B) and Nitrogen (N) composition. The constituents of the synthesized sample are displayed *via* different peaks in the XPS survey shown in Fig. 3. The survey shows several peaks at 190.3, 193, 398 and 533 eV. The B1s peak at 190.3 eV and N1s peak at 398 eV stand for the h-BN nature of the BNNTs.[25,26] The peak at 193 eV refers to the existence of B_2O_3 in the sample that might have formed as an impurity during the synthesis of BNNTs.[27] The O 1 s peak reported at 533 eV may either be due to the as-used Si-substrate, exposure of sample in the air[28] or B_2O_3.

Raman spectroscopy is used to further confirm B and N components and the h-BN phase of the synthesized BNNTs. The Raman spectrum obtained during the Raman spectroscopy of the synthesized BNNT sample is shown in Fig. 4. The components of the sample are recognized from the reported peaks in the Raman spectrum. The Raman spectrum in Fig. 4 shows major peaks at 1370 (cm^{-1}) for the main compositions of the sample and a smaller intensity peak at 1128 (cm^{-1}) for a minute quantity of impurity in the final product. The major peak corresponds to E_{2g} mode of vibration in h-BN,[18] whereas the smaller intensity peak reports the formation of boric acid which might be due to the interaction of laser with moisture, B_2O_3 left in the sample and oxygen in the air.[29]

Initially, Argon gas is used as a reaction atmosphere from room temperature to 1200 °C. Argon gas is found to stay for one hour inside the chamber after it has been switched off.[30] At 1200 °C, Argon is replaced by NH_3 gas flow for 180 min. During the first hour (in the presence of the Argon gas inert atmosphere), the reaction parameters resulted in the synthesis of smaller diameter (70–130 nm) BNNTs.[21] In the presence of Argon, almost all the NH_3 introduced ito the system is decomposed into nitrogen and hydrogen. Nitrogen is utilized in the formation of BN-species, whereas, Argon due to its anti-oxidant nature prevents the formation of water vapor and allows the hydrogen to be burnt to provide extra energy for the growth of the BNNTs. It might be the possible reason for why all the BNNTs grown during this stage have a uniform diameter.

At the end of the first hour and the start of the second hour there are still plenty of growth species (B_2O_2) available.

These growth species rapidly react with N_2 from the decomposed portion of NH_3 (the non-decomposed NH_3 works as a reaction atmosphere and takes away the undesired morphologies outside the reaction chamber) and form BN-species. The lack of an inert atmosphere results in a decrease in the mean free path. The decrease in the mean free path causes most of the BN-species to get stuck with a nearby BNNT and results in an enormous increase in its diameter. This process continues till all the growth species are converted into BN-species and stuck with the BNNTs. A time comes when the precursors are blocked by the synthesized BNNTs in the boat that prevents the formation of further growth species. At the end of the second hour and start of the third hour, no more growth species are formed due to the blockage of precursors in the boat. During this stage, nitrogen from decomposed NH_3 works as a reaction atmosphere (alongside with non-decomposed NH_3) whereas hydrogen burns in the same atmosphere and provides extra heat energy. This situation causes another stage of BNNT growth with a pipe like morphology that can clearly be seen in the FESEM micrograph shown in Fig. 1(c).

4. Conclusions

The results obtained in the present work suggest that the growth duration and the reaction atmosphere during the growth has a key role in determining the size and final morphology of boron nitride nanotubes. Smaller diameter nanotubes in the range of 70–130 nm can be synthesized in the presence of the Argon gas inert atmosphere, whereas larger diameter nanotubes in the range of 70–700 nm and above can be synthesized in the presence of ammonia as a reaction atmosphere. Similarly, the appearance of nitrogen (with excess heat enegry due to hydrogen burning) at the last stage of the experiment starts further growth of the nanotubes with a clear pipe-like morphology.

Thus, the present work provides an opportunity to material scientists and researchers to grow boron nitride nanotubes of desired size and morphology by only changing the reaction atmosphere and growth duration within a single experiment, using the same experimental set up and precursor type. This will further be a step toward the commercialized production of boron nitride nanotubes or other hexagonal boron nitride nano-products for their potential applications in the field of bio-medicine, microelectronic mechanical systems and solid state neutron detectors.

References

1 S. Iijima, *Nature*, 1991, **354**, 56–58.
2 M. Ishigami, S. Aloni, A. Zettl, AIP Conference Proceedings, 2003, pp. 94–99.
3 X. Blase, A. Rubio, S. G. Louie and M. L. Cohen, *Europhys. Lett.*, 1994, **28**, 335–340.
4 N. G. Chopra, R. Luyken, K. Cherrey, V. H. Crespi, M. L. Cohen, S. G. Louie and A. Zettl, *Science*, 1995, **269**, 966–967.
5 J. Wang, C. H. Lee and Y. K. Yap, *Nanoscale*, 2010, **2**, 2028–2034.
6 M. Liao and Y. Koide, *Crit. Rev. Solid State Mater. Sci.*, 2011, **36**, 66–101.
7 P. Ahmad, M. U. Khandaker and Y. M. Amin, *Ceram. Int.*, 2015, **41**, 4544–4548.
8 B. Akdim, R. Pachter, X. Duan and W. W. Adams, *Phys. Rev. B: Condens. Matter Mater. Phys.*, 2003, **67**, 245404.
9 B.-C. Wang, M.-H. Tsai and Y.-M. Chou, *Synth. Met.*, 1997, **86**, 2379–2380.
10 A. Leela Mohana Reddy, A. E. Tanur and G. C. Walker, *Int. J. Hydrogen Energy*, 2010, **35**, 4138–4143.
11 G. Mpourmpakis and G. E. Froudakis, *Catal. Today*, 2007, **120**, 341–345.
12 S. Hu, E.-J. Kan and J. Yang, *J. Chem. Phys.*, 2007, **127**, 164718.
13 S. Shevlin and Z. Guo, *Phys. Rev. B: Condens. Matter Mater. Phys.*, 2007, **76**, 024104.
14 E. Durgun, Y.-R. Jang and S. Ciraci, *Phys. Rev. B: Condens. Matter Mater. Phys.*, 2007, **76**, 073413.
15 Q. Huang, Y. Bando, X. Xu, T. Nishimura, C. Zhi, C. Tang, F. Xu, L. Gao and D. Golberg, *Nanotechnology*, 2007, **18**, 485706.
16 P. Ahmad, M. U. Khandaker, Z. R. Khan and Y. M. Amin, *Ceram. Int.*, 2014, **40**, 14727–14732.
17 C. Zhi, Y. Bando, C. Tan and D. Golberg, *Solid State Commun.*, 2005, **135**, 67–70.
18 C. H. Lee, J. S. Wang, V. K. Kayatsha, J. Y. Huang and Y. K. Yap, *Nanotechnology*, 2008, **19**, 455605.
19 C. H. Lee, M. Xie, V. Kayastha, J. S. Wang and Y. K. Yap, *Chem. Mater.*, 2010, **22**, 1782–1787.
20 A. Pakdel, C. Zhi, Y. Bando, T. Nakayama and D. Golberg, *Nanotechnology*, 2012, **23**, 215601.
21 P. Ahmad, M. U. Khandaker and Y. M. Amin, *Phys. E*, 2015, **67**, 33–37.
22 P. Ahmad, M. U. Khandaker, Y. M. Amin and Z. R. Khan, *Mater. Manuf. Processes*, 2014, **30**, 184–188.
23 P. Ahmad, M. Khandaker and Y. Amin, *Adv. Appl. Ceram.*, 2015, **114**, 267–272.
24 P. Ahmad, M. U. Khandaker and Y. M. Amin, *Indian J. Phys.*, 2015, **89**, 209–216.
25 S. Sinnott, R. Andrews, D. Qian, A. Rao, Z. Mao, E. Dickey and F. Derbyshire, *Chem. Phys. Lett.*, 1999, **315**, 25–30.
26 C.-Y. Su, W.-Y. Chu, Z.-Y. Juang, K.-F. Chen, B.-M. Cheng, F.-R. Chen, K.-C. Leou and C.-H. Tsai, *J. Phys. Chem. C*, 2009, **113**, 14732–14738.
27 C. D. Wagner, *Physical Electronics Division*, Perkin-Elmer Corp., 1979.
28 B. Zhong, L. Song, X. X. Huang, G. W. Wen and L. Xia, *Mater. Res. Bull.*, 2011, **46**, 1521–1523.
29 R. Arenal, A. C. Ferrari, S. Reich, L. Wirtz, J. Y. Mevellec, S. Lefrant, A. Rubio and A. Loiseau, *Nano Lett.*, 2006, **6**, 1812–1816.
30 D. Özmen, N. A. Sezgi and S. Balcı, *Chem. Eng. J.*, 2013, **219**, 28–36.